ARCHITECTURAL SCIENCE REVIEW
https://doi.org/10.1080/00038628.2024.2381715

Taylor & Francis
Taylor & Francis Group

Development and thermal performance testing of radiant conditioning ceiling panels

Hung Q. Do[a], Jane Matthews[a], Mark B. Luther[b], Igor Martek[a] and Peter Horan[a]

[a]School of Architecture and Built Environment, Deakin University, Geelong, Australia; [b]Environmental Energy Services Pty. Ltd, Moolap, Australia

ABSTRACT

The past decades have seen an advancement from heavyweight radiant floors to lightweight conditioning ceiling systems. However, the performance of these lightweight systems are seldom comprehensively discussed in an informative manner for designers. This paper reviews lightweight radiant ceiling panel designs and conducts instrumental experiments to examine the thermal performance of different designs. Four distinct capillary hydronic panels have been designed and developed to assesses their thermal performance via empirical testing and measurement. Prototypes were built and integrated into a suspended ceiling system where they were tested in cooling mode. The response time, surface temperature, and energy transfer of the different panel designs were investigated. The experiment results show that higher thermal mass yields higher heat transfer and better surface temperature, but longer response time. A better thermal connection between the capillary tubes and the radiant surface also results in better conduction, faster response times, and improved surface temperature.

ARTICLE HISTORY
Received 29 January 2024
Accepted 12 July 2024

KEYWORDS
Thermal performance; cooling capacity; lightweight radiant systems design; heat flux; time constant; heat transfer

1. Introduction

Applying radiant conditioning systems is a potential solution for providing thermal comfort with low energy consumption (Rhee and Kim 2015). Radiant systems can be used as supplements, working in conjunction with conventional convective systems to provide thermal comfort (Rhee, Olesen, and Kim 2017). Usually, more than 50% of the conditioning load provided by a planer radiant conditioning system is radiant heat transfer (Rhee and Kim 2015). In short, radiant systems control mean radiant temperature (MRT) as well as air temperature. Recently, radiant conditioning systems have gained popularity due to their advantages over their convective counterparts, in particular energy-saving potential, improved thermal comfort, reduced draught risk, and quieter operation (Rhee and Kim 2015).

In Australia, conditioning systems account for about 39% of the energy used in a typical commercial building (Residovic 2017). It is anticipated that 25% of Australia's targeted greenhouse gas emissions reduction by 2030 needs to be accounted for through building energy efficiency improvement (Bulut et al. 2021). Applying radiant conditioning may be a viable option for improving thermal and energy performance in commercial buildings in Australia (Do et al. 2022a; 2022b). Commercial buildings in Australia can be retrofitted with radiant systems, especially at perimeter zones in office buildings where thermal building loads fluctuate widely and mean radiant control is required (Anderson, Luther, and Brain 2011; Anderson and Luther 2012; Luther, Tokede, and Liu 2020). However, the number of applications on radiant systems from Australian researchers is not notable (Rhee and Kim 2015). At the same time, many radiant systems currently used in Australia are imported directly from Europe while their performance in some dynamic climatic conditions of Australia is not well-studied. Presently, the Australian market applies wet (concrete), heavyweight systems, not suitable for retrofitting existing buildings. Hence, our study proposes designs for ceiling radiant panels that meet these needs for the Australian market.

To date, the research conducted on different configurations for radiant panel designs has focused on improving capacity while preventing condensation during cooling. One of the most notable limitations of radiant systems is their limited cooling capacity (Babiak, Olesen, and Petras 2007). The two main reasons for this are; the risk of condensation (Babiak, Olesen, and Petras 2007; Xing et al. 2021) and low heat transfer efficiency between the chilled water and the room (Yin et al. 2014). Firstly, the cooling capacity of radiant cooling panels relies on low surface temperature. The lower the surface temperature the higher the cooling capacity. However, the surface temperature must remain higher than the due point to prevent condensation thus limiting the capacity. In high-humid conditions, the due point gets closer to the air (dry bub) temperature and further limits the cooling capacity of radiant systems. To tackle the condensation problem, researchers have been promoting solutions including drainage and dehumidification systems (Zhong et al. 2022). Furthermore, there are two passive solutions namely changing the texture of the radiant surface to prevent condensation and create a uniform surface temperature (Xing and Li 2022).

CONTACT Jane Matthews jane.matthews@deakin.edu.au School of Architecture and Built Environment, Deakin University, Geelong, VIC, Australia 3220

Following the first strategy, Zhong et al. (2022) propose superhydrophobic surfaces on metal cooling panels and successfully mitigate condensation while achieving 209 W/m^2 with a 20°C difference between the ambient and radiant surface temperature. The authors explained that the only limitation of this solution is ensuring the consistency and durability of the superhydrophobic surface on a practical production scale. Morse (1963) promoted a cooling panel design with a polyethylene sheet shielding the radiant surface from the ambient air so that the panel can be operated below the dew point. The design was improved by Teitelbaum et al. (2020) resulting in a system capable of providing adequate radiant cooling in an open space in the hot humid climate of Singapore with no condensation. However, questions can be raised about the practicality of such a design with unusually high panel thickness and fragile membrane. Yin et al. (2014) use gypsum as the radiant surface instead of smooth metal resulting in higher capacity and condensation prevention for the gypsum board. This seems to be a practical solution and inspires some panel designs in this sudy although the heat transfer coefficient of gypsum board can be questionable.

The second strategy is to obtain a uniform surface temperature across the radiant panel ensuring high heat flux while keeping the cooling surface above the dew point. As the surface temperatures are limited above the dewpoint, the ununiform surface temperatures provide hotter temperatures and lower heat flux in some areas, reducing total heat transfer capacity. Using simulation, Xing and Li (2022) proposed a new piping system for radiant panels that results in a more uniform surface temperature allowing 4°C hotter inlet cooling water to have the same cooling capacity, or increasing cooling capacity while the radiant surface temperature remains higher than the dewpoint. Empirical experiments have yet to be conducted on this highly potential design. Ye et al. (2023), promoted a strategy of reducing the pipe spacing in radiant panels to improve surface temperature uniformity to increase heat transfer and prevent condensation although such a solution can be costly.

Low heat transfer efficiency between the system and the room is mentioned in several publications such as the REHVA handbook (Babiak, Olesen, and Petras 2007), the research of Yin et al. (2014), and Xing and Li (2022). It is desired for the materials of the radiant panel to have high thermal conductivity to ensure heat transfer between the panel surface and the room. The heat transfer between water tubes and the surface as well as the surface and room determines the performance of the panels. The effect of material property, panel design, type of thermal connection, and thermal mass of the panel requires further investigation.

The main purpose of this study is to investigate the connection between radiant panel designs and their thermal performance including cooling capacity, time constant, and heat transfer coefficient. To do so, this research achieved three objectives, proposing four designs of capillary mat radiant panels, conducting instrumental experiments on the panels, and comparing their thermal performance and properties against each other. These results are potential panel designs, improvement in panel design and applied materials, as well as developing an understanding of radiant panels in general.

2. Radiant panel design

2.1. Types of radiant cooling ceiling

Presently, There are three types of radiant systems; Radiant Panels (RP), Embedded Surface Systems (ESS), and Thermal Active Building Systems (TABS) (Babiak, Olesen, and Petras 2007). Among them, Radiant Panels (RP) (Figure 1) stand out for being lightweight, easier to control, and more responsive than the other systems (Babiak, Olesen, and Petras 2007; Feng 2014; Imanari, Omori, and Bogaki 1999; Miriel, Serres, and Trombe 2002).

Embedded surface systems (ESS) are also commonly used for radiant ceilings (Babiak, Olesen, and Petras 2007). Figure 2 shows ESS system types A and B for radiant ceilings. Type A is a 'wet' system with the pipes embedded inside the finishing layer while Type B is a 'dry' system with pipes 'touching' the finished surface, usually drywall.

Figure 3 shows an application of a Type B radiant ceiling installed in a housing project in Australia with capillary tube mats sitting on a dry gypsum ceiling (Point A) and insulated with wool blankets (Point B).

2.2. Piping in radiant ceiling

Hydronic piping in radiant systems can be divided into two categories: those using Ø10–20 mm tubes (metal or plastic), and those using polypropylene capillary tube mats (Díaz and Cuevas 2010). Figure 4(A) and (B) show a radiant system with copper tubes and capillary tube mats, respectively. The radiant systems with capillary tube mats have been proven to have superior performance, especially in terms of surface temperature uniformity (Ding et al. 2020; Jing and Jiayu 2020). Additionally, the capillary tube mats provide flexibility in design and installation, although the tubes can easily be blocked by air bubbles (Miriel, Serres, and Trombe 2002). To tackle the air blockage, bubbles must be forced out of the system via degassing measures such as pressure relief valves. Consequently, capillary radiant systems are usually operated in closed-loop and require pressurization to ensure an unrestricted flow rate and prevent bubbles from clogging up the piping.

Figure 5 shows two types of flow channels commonly used in capillary tube mats. In principle, water circulation requires an equal path length throughout all of the capillary tubes and manifold in the mat. The flow channel of water through the panel plays a critical role in the thermal performance of the panel (Mosa, Labat, and Lorente 2019a; 2019b). For example, Figure 5(A) shows a capillary tube mat with the '*U*-turn' while the mat in Figure 5(B) is with the 'canopy-to-canopy' flow channel design.

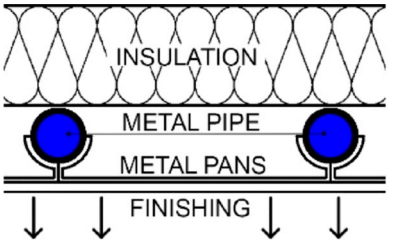

Figure 1. A common radiant ceiling panel system.

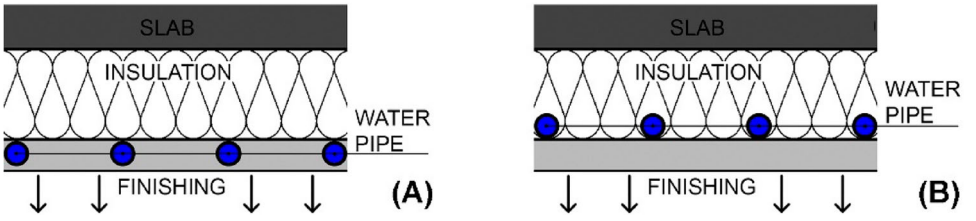

Figure 2. (A) Type A ESS; (B) Type B ESS.

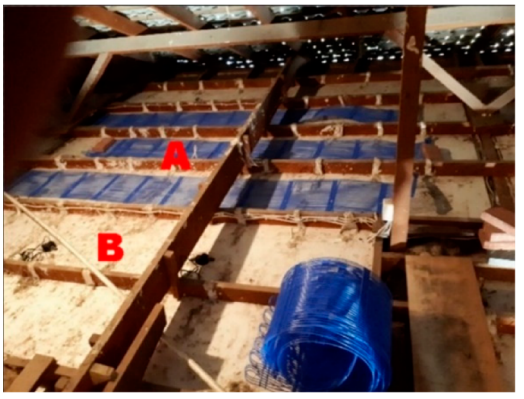

Figure 3. Radiant ceiling being installed in a housing project in Australia.

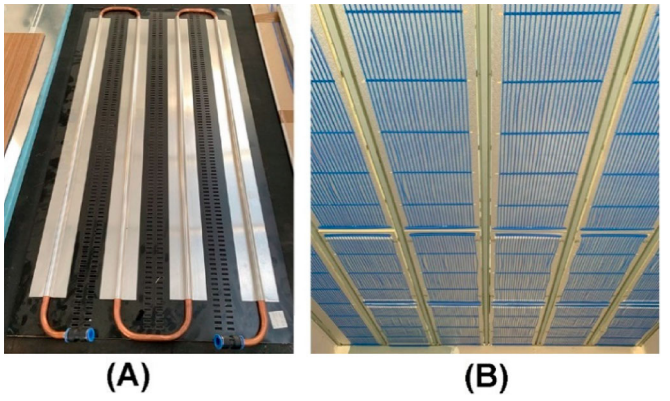

Figure 4. (A) a radiant system with metal tubes (Ø15 mm); (B) a radiant system with capillary tube (Ø4 mm) mats.

Among them, the 'canopy-to-canopy' design has the least resistance to flow and shorter flow distance. Applying the 'canopy-to-canopy' flow channel can result in a more uniform surface temperature for the radiant panels (Mosa, Labat, and Lorente 2019a; 2019b). Therefore, we selected the 'canopy-to-canopy' design for our test panels.

2.3. Key components

Four designs for radiant panels are proposed in this research each capable of being integrated into a commonly used suspended ceiling frame with ease (panel dimensions 590 × 1190 mm) (Figure 6A). A rigid insulation board was chosen for its lightweight, readily available, and high *R*-value. The insulation board consists of a 25 mm thick polyisocyanurate foam (PIR) panel, with two reflective aluminum layers (Figure 6B). The *R*-value of the insulation is 1.05 m^2K/W. While easy to work with, the insulation is highly durable and can support the structure of the radiant panels. The capillary tube mats measure 550 × 1150 mm and readily fit within the panels (Figure 6C). Each mat weighs 0.5 kg (empty) and can contain about 0.45 L of water.

2.4. Panel design

Design 1 is shown in Figure 7(A). Plaster-based ceiling tiles are used as the radiant surface. Grooves were routed on the back side of the plaster-based ceiling tile to accommodate the capillary tubes, thus partially embedding them inside the tile. This is similar to the 'ESS type A' radiant ceiling design, shown in the REHVA handbook (Figure 2A) (Babiak, Olesen, and Petras 2007). Design 1 is also a dry system, easy to assemble and install. The radiant surface, the tube mat, and the insulation board are glued together to create one unified panel. The final panel weighs 6 kg without water.

Figure 7(B) shows Design 2. Here the capillary tubes are not embedded in the plasterboard but sandwiched between the ceiling tile and the rigid insulation board. Hence, the tube mat only 'touches' the radiant surface. This is similar to the radiant ceiling (Figure 3), and the ESS type B design (Figure 2B) but the capillary tubes are not embedded inside the insulation. This panel is slightly heavier than panel 1, weighing 6.5 kg.

In Design 3, a plaster-based ceiling tile is also used as the radiant surface. Here the insulation board, capillary tube mat, and radiant surface are bonded together with gypsum mortar (Figure 7C). Design 3 is similar to Design 1, embedding the capillary tubes inside the radiant surface, although it is heavier and is a wet system. Hence this design can be considered a variant of 'ESS type A' (Figure 2A). This is the heaviest panel weighing 10 kg.

Design 4 (Figure 7D), is similar to Design 2, but here the radiant surface is a perforated metal sheet. The metal sheet is light and has low thermal resistance making it an ideal radiant surface. A similar design was also tested by Yin et al. (2014). Their results show that if the metal sheet is not properly connected to the capillary tube mat, the performance of the panel is significantly hindered. Hence, metal pins and rivets were used to firmly 'press' the metal sheet against the tubes for improved heat transfer. Panel 4 is the lightest, weighing only 3.5 kg. Hence, more experimental designs for a better connection are necessary.

3. Methodology and data collection

3.1. Research methodology and design

The objective of this section of our paper is to introduce and make aware to the readers the analytical processes for

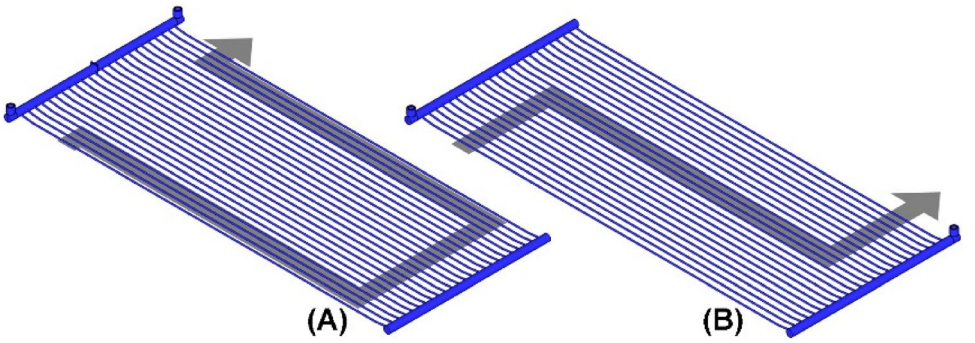

Figure 5. (A) '*U*-turn' flow tube mat; (B) 'canopy-to-canopy' flow tube mat.

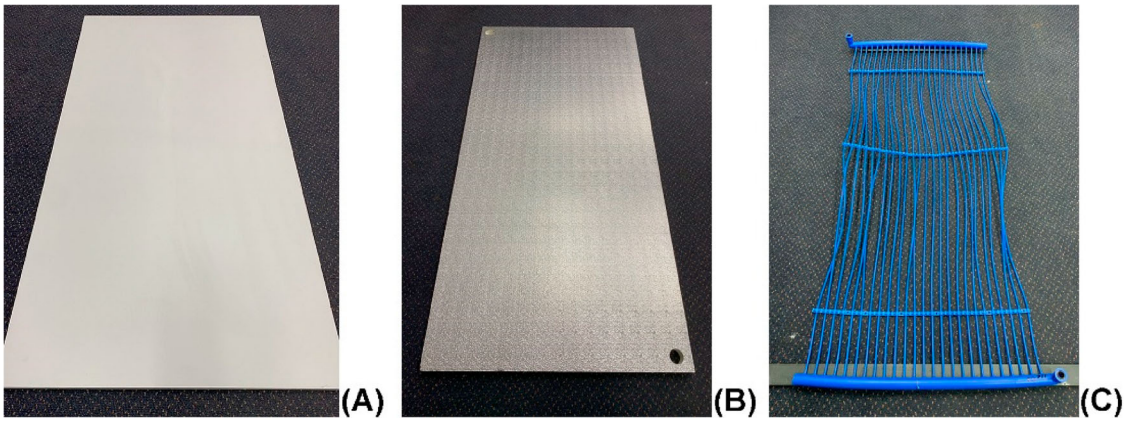

Figure 6. (A) Ceiling tile 1200 × 600 mm; (B) Insulation board; (C) Capillary tube mat.

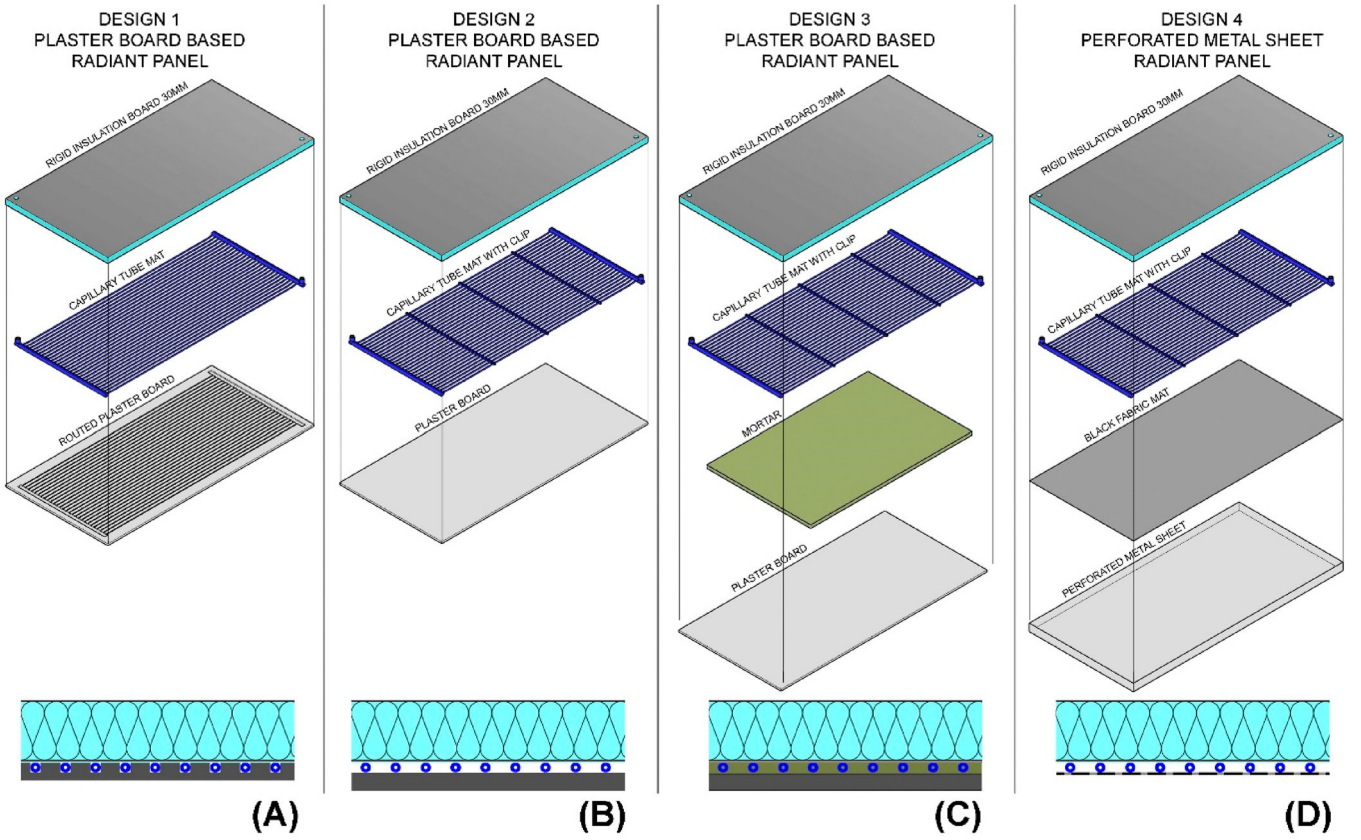

Figure 7. Four radiant ceiling panel designs.

evaluating and improving hydronic radiant panel system performance. Quantitative parameters regarding the panels' properties and performance were measured directly via instrumental experiments as well as numerical calculations. Relative comparison analyses were conducted to compare the panels' thermal performance and evaluate the effectiveness of the panel designs. Qualitative aspects such as design complexity or ease of panel building were also used for further comparison.

3.2. Parameters to be measured and calculated

The data gathered measures three aspects of the thermal performance of the prototypes, namely radiant surface temperature, time constant, and heat transfer (heat flux). The heat flux sensor can read the total heat transfer (q) including convective (q_c) and radiant (q_r) heat transfer between the radiant surface and the conditioned space. Heat transfer along with surface temperature are crucial factors determining the conditioning capacity of radiant systems (Babiak, Olesen, and Petras 2007). The operative temperature of the test environment is calculated based on the air and black-globe temperature. The radiant system operation parameters such as inlet water temperature, outlet water temperature as well as water flow rate are also measured. The measured parameters allow the heat transfer coefficient and the thermal transmittance or the thermal resistance of the panel structure to be calculated. Table 1 below shows the parameters to be measured and calculated in this study.

3.3. Panel heat transfer and heat transfer coefficient

The heat transfer between the panels and the conditioned space is the result of the temperature difference between the surface and the operative temperature of the conditioned space. The relationship between heat flux and temperature difference between the radiant surface and the conditioned room is indicated by the equation below (Babiak, Olesen, and Petras 2007).

$$q = h_t(OT_i - T_S) \tag{1}$$

Where:

- q is the total heat flux (W/m^2)
- h_t is the total heat transfer coefficient (W/m^{2}K)
- OT_i is the ambient operative temperature (°C or K)
- T_s is the radiant surface temperature (°C or K)

Table 1. Parameters to be measured and calculated.

Parameter	Symbols	Unit	Collection
Radiant surface temperature	T_S	°C or K	Thermocouple
Heat flux (heat transfer)	q	W/m^2	Heat flux sensor
Heat transfer coefficient	h_t	W/m^{2}K	Calculation
Time constant	TC	Minute	Calculation
Thermal transmittance of the panel structure	U_t	W/m^{2}K	Calculation
Operative temperature	OT_i	°C or K	Calculation
Inlet water temperature	T_i	°C or K	Thermocouple
Outlet water temperature	T_o	°C or K	Thermocouple
Water flowrate	Q	L/min	Flowmeter

The total heat transfer coefficient is the sum of radiant and convective heat transfer coefficients:

$$h_t = h_c + h_r \tag{2}$$

Where:

- h_c is the convective heat transfer coefficient (W/m^{2}K)
- h_r is the radiant heat transfer coefficient (W/m^{2}K)

The calculation method for radiant heat transfer coefficient (h_r) is shown in detail in the research of Cholewa et al. (2017) and is quite complex. However, the RHEVA handbook (Babiak, Olesen, and Petras 2007) provides the value of heat transfer coefficients of various radiant systems. In normal operating conditions, the radiant heat transfer coefficient (h_r) of a radiant system is fixed at 5.5 W/m^{2}K regardless of conditioning mode or mounting position (e.g. floor, wall, or ceiling) (Babiak, Olesen, and Petras 2007; Shinoda et al. 2019). This value for a radiant heat transfer coefficient (h_r) is widely agreed upon among researchers (Shinoda et al. 2019). The convective heat transfer coefficient (h_c) can vary based on the conditioning mode (heating or cooling), mounting position (wall, floor, ceiling), and air velocity (forced convection). The total heat transfer coefficient (h) suggested in the RHEVA handbook of a cooling ceiling panel is 11 W/m^{2}k. Similar values are suggested by the EN1264-5 and EN15377-1 standards (Shinoda et al. 2019). However, several publications suggest the total heat transfer coefficient (h) of the cooling ceiling can be lower, 8–10 W/m^{2}K depending on ventilation, room size, heat source, etc (Shinoda et al. 2019).

Furthermore, the radiant surface temperature is primarily the result of the heat transfer between the water and the panel materials. Here, inlet and outlet water temperature and flow rate play a critical role in the rate of energy transfer to the radiant panel surface. As the panels are designed so that most of the heat transfer between the water and panel is directed toward the conditioned room, the heat flux can be calculated using Equation (3) below:

$$q = m * C * (T_o - T_i)/(S * t) \tag{3}$$

Where:

- m is the mass of the water flow through a panel (kg)
- C is the specific heat capacity of water (4182 J/kgK)
- T_i is the inlet water temperature (°C or K)
- T_o is the outlet water temperature (°C or K)
- S is the area of the panel (m^2)
- t is the time of the measurement (s)

3.4. Thermal transmittance (U-value) of the panel structure

While the aforementioned method (Equation 3) allows the calculation of heat flux via water flow rate and temperatures, it is a method of indirect measurement that may have low accuracy as several assumptions are required (Cholewa et al. 2017). Meanwhile, the whole cooling process relies upon the heat transfer between the cold water and the room through the conducting surface of the panels. The effectiveness of heat transfer is

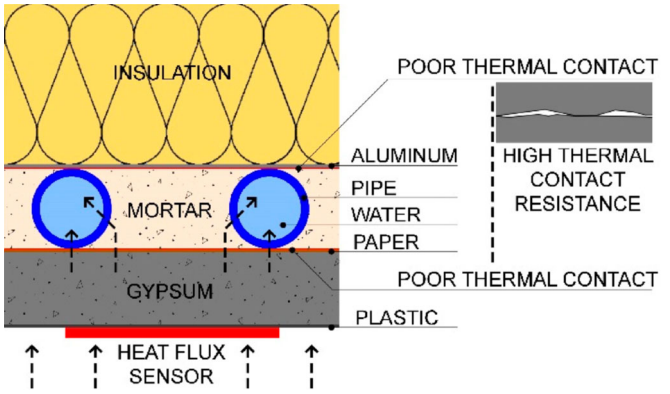

Figure 8. A panel composition indicating locations of thermal contact resistance.

reliant upon the materials selected throughout the panel. It can be assumed that most of the heat transfer between the water and the panel radiant surface will then transfer to the room.

$$q = (T_s - T_w)U_t \tag{4}$$

Where:

– U_t is the total *U*-value (Thermal transmittance) of the panel material structure (W/m^{2}K)
– T_s is the temperature of the radiant surface (°C or K)
– T_w is the average of the water temperature inside the panel (°C or K)

The total *U*-value of the panel composition is inclusive of the materials between the water and the radiant surface itself. Xing and Li (2022) explained that the components of the radiant panel are designed to touch/contact each other and the imperfection/inefficiency of such thermal connection is the reason for high thermal contact resistance which can hinder the performance of radiant panels. Figure 8 shows the composition of a panel where several different materials interact causing thermal contact resistance. Hence the total *U*-value (the mathematical inverse of the *R*-value) of a panel indicates how efficiently the panel can transfer heat through its composition (Díaz and Cuevas 2010). Panels with higher *U*-value will perform better, and represent more conduction through the entire panel system.

3.5. Time constant

The following equation can be used to determine the time constant.

$$y = (initial\ value - final\ value) * e^{-t/TC} + final\ value \tag{5}$$

Where:

– TC is the time constant (minute)
– *t* is the time between changes (minute)

Equation (5) provides a mathematical model for the reaction time of the panel. Here, heat flux indicates the operation hence the time constant of these parameters indicates how fast the systems respond. The time constant (TC) of heat flux and surface temperature is the time needed for each parameter to reach 63.21% of its maximum range (Ning, Schiavon, and Bauman 2015). Figure 9 shows the heat flux of panel 1 in a preliminary test run. The initial heat flux is 0 W/m^2, the maximum heat flux is 86 W/m^2 and the time interval is one minute. These values were applied to the equation, with a time constant of 10, 15, and 20 min, and superimposed over the heat flux (Figure 9). The time constant of 15 min closely matches the heat flux of panel 1. The same process was applied to the readings of the other panels.

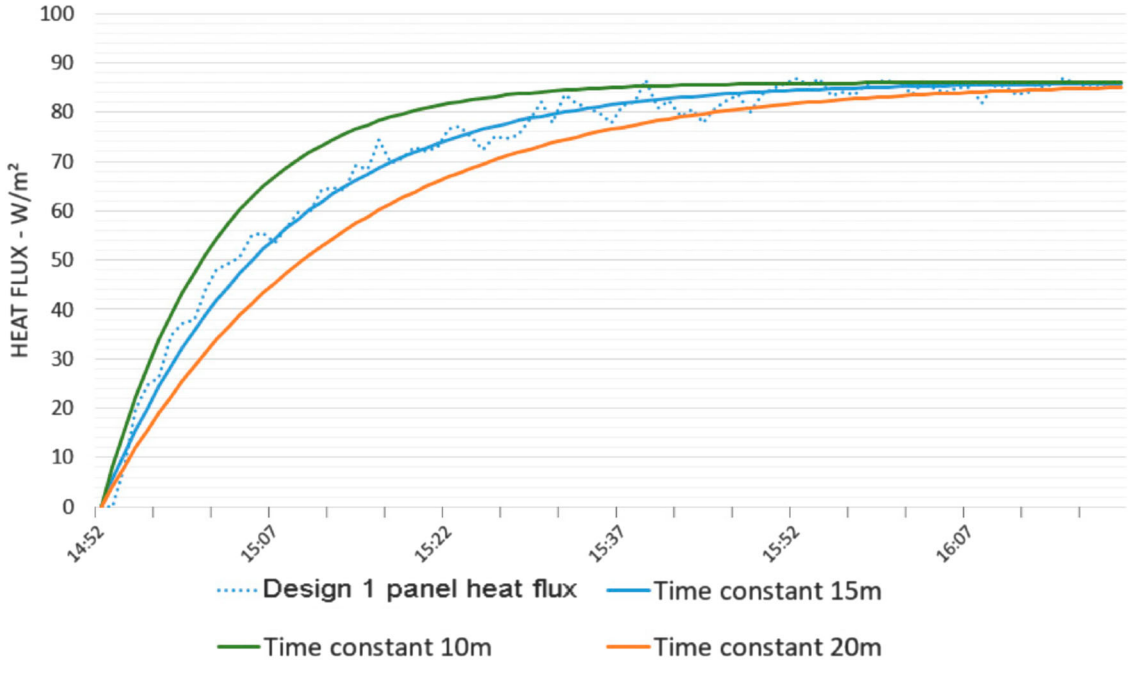

Figure 9. An example of different time constant models applied to Design 1 panel.

3.6. Data analysis

Relative comparative analyses were conducted to compare the thermal performance and properties of the prototype panels. The heat flux and surface temperature were measured for each panel as the main data for performance analysis (Xing and Li 2022). In our study, the inlet water temperature for each panel is the same, hence panels with higher heat transfer between the water and the radiant surface have higher heat flux and better (lower) surface temperatures. As the system is started and pumps cold water through the panels, the heat exchange process is initiated. The surface temperature of the panels decreases and the heat flux rises until it reaches a maximum reading. This inverse relationship between the heat flux and surface temperature can be used to validate the readings.

The time constant (TC) is an important parameter determining how fast a system responds to a change or a control command (Yu and Yao 2015; Ye et al. 2021). A high response time causes difficulties in system control, low energy efficiency, and increased discomfort (Babiak, Olesen, and Petras 2007). Hence, we are aiming for systems with faster response times. The time constant of a panel in a test run was calculated using Equation (5).

The thermal transmittance (*U*-value) of the panel composition was calculated via Equation (4). A higher *U*-value indicates better heat transfer between the water and the radiant surface and results in higher thermal performance (Xing and Li 2022).

4. Instrumental experiment

4.1. Equipment and sensors

Table 1 shows the equipment used to collect the required data. Four FHF05 foil heat flux sensors were used to collect the heat flux data. These heat flux sensors are supplied pre-calibrated and certified. Additionally, the readings of the sensors were cross-checked through the preliminary experiments to ensure consistent and accurate reading results. The thermocouples were also calibrated using a Dobros Precision mercury thermometer to ensure below 0.5°C error.

A thermal imaging camera (AVIO Neo Thermo TVS-700) was used to assist the heat flux sensor and identify any air blockages. A thermal comfort cart with built-in thermocouples and black globe temperature sensors was used to measure the ambient operative temperature. The water flow rate and the inlet water temperatures were monitored by a digital flow metre on the hydronic control panel of the system. Eight thermocouples were applied to the inlet and outlet points of the panels to measure the inlet and outlet water temperatures.

4.2. Experiment setup

All of the panels are integrated into one ceiling system that ensures equal water flow rate and inlet temperature into each panel. The experiment is set up in an industrial shed to emulate an open office space and is protected from external weather conditions especially air velocity which can affect the convective heat transfer (q_c) between the panels and the space.

Figure 10 shows the experiment setup. At the centre of each panel, a heat flux Hukseflux FHF05 sensor is attached. The sensors are connected to a Campbell Scientific CR10X data logger for data collection and storage. The digital flow metre is attached to the water supply hose at the hydronic control panel. Eight thermocouples are applied to the inlet and outlet points of the panels. Data from these thermocouples are also collected using a Campbell Scientific CR10X. The air and black globe temperature data from the Comfort Cart is collected and stored in a Campbell Scientific CR23X.

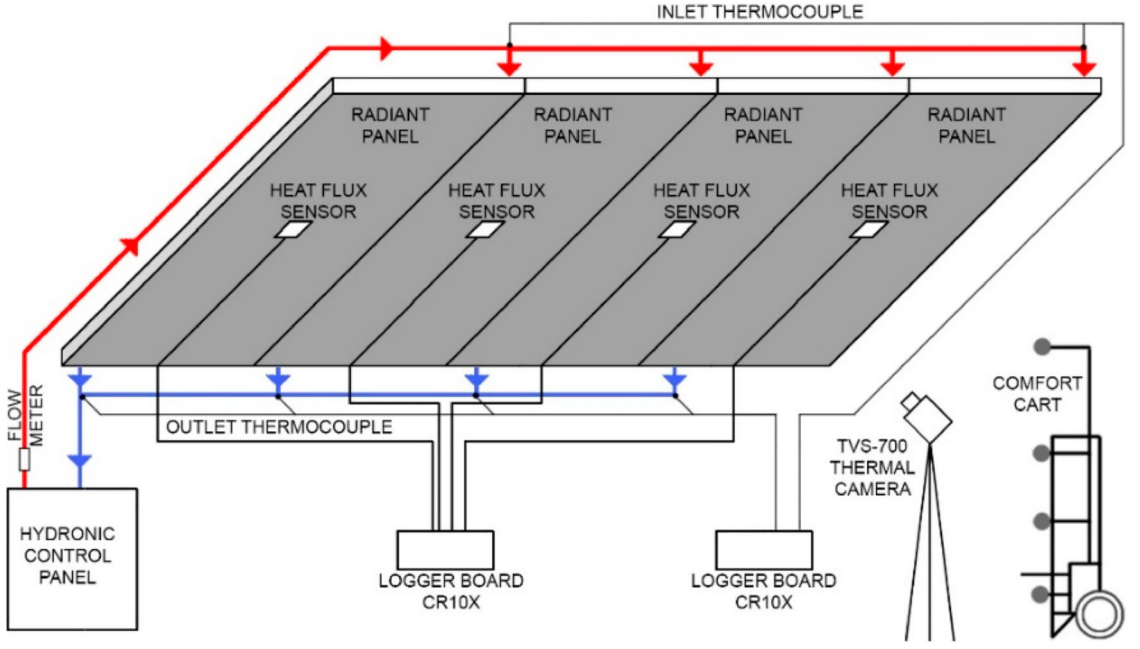

Figure 10. Experiment setup of the four ceiling panel designs.

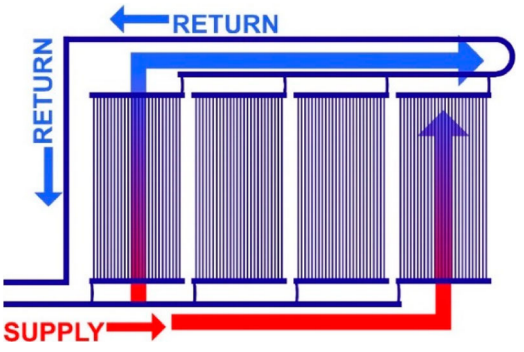

Figure 11. 'Canopy to canopy' design, showing equal distances of the flow path for each panel.

This experiment setup is similar to experiments conducted by Gallardo and Berardi (2022) and Li et al. (2015) on radiant cooling ceilings with the heat flux sensor attached to the centre of the radiant panel. Li et al. (2015) used a thermal camera to monitor the ceiling panels to find the most representative position for heat flux sensor attachment. The centre of the panel was chosen as the surface temperature at the centre was found to be close to the average temperature of the panel surface. In this study, the recorded thermographs show that the surface temperature is relatively uniform across the central panel area where the capillary mat is located. The temperature changes also seem to be uniform in the central area of the panels. Notably, the cooling effect is not present at the edge of the panels. As a consequence, the heat flux sensors were placed at the centre of each of the panels.

The same 'canopy-to-canopy' flow channel design is also applied to the whole system when the 4 prototype panels are hooked up parallel to each other (Figure 11). The aim is to ensure an equal pathway of water supply throughout all panels. To achieve this, the distance (length of piping) must be equal for each panel connected to the supply side as well as the return side. Associated with this arrangement, all of our panels can be tested with equal input conditions. This allows a fair and consistent comparative analysis of the thermal performance of the panels.

4.3. Experiment principle

The panels were tested in a cooling mode, as radiant ceiling systems are mainly used for radiant cooling. Hence test runs were conducted on hot days (sunny and above 26°C) between 10 AM and 5 PM. The heat pump was turned on prior to the test run to produce cold water (around 10°C) and was kept running during the experiment. At the start of a test run the pump and all the valves on the hydronic control panel were opened to supply cold water to the ceiling and activate the flowmeter. In all test runs the system was operated at full capacity. After at least three hours running, the system was shut down including the heat pump, water pump, and all of the valves ensuring no cooling supply to the ceiling. The sensors (heat flux and thermocouple) monitor the condition of the panel before, during, and after the experiment, and collect and store the data in loggers. The data points chosen for analysis are between 15 min before the system is turned on to 1.5 h after the system is turned off.

5. Experiment results

5.1. Heat flux and surface temperature

Several test runs were conducted under different ambient conditions. Each of the panel types demonstrated a consistent outcome for heat flux output across the test runs. Figure 12 shows the heat flux of the four panels during a typical test run. Design 1 performed best, yielding the highest heat flux readings of the four subject panels reaching 95 W/m^2. Design 3 was the second best yielding 85–90 W/m^2. Ranked third, the heat flux readings of Design 4 reached around 80 W/m^2. Interestingly, the heat flux values yielded by these three panels are relatively close to

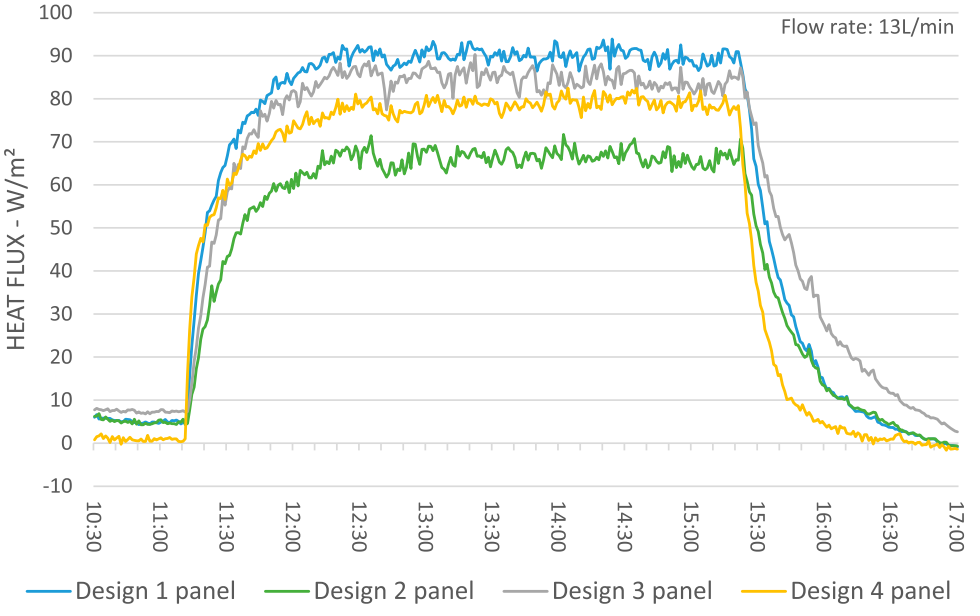

Figure 12. Heat flux output of the four ceiling panel designs in an experiment.

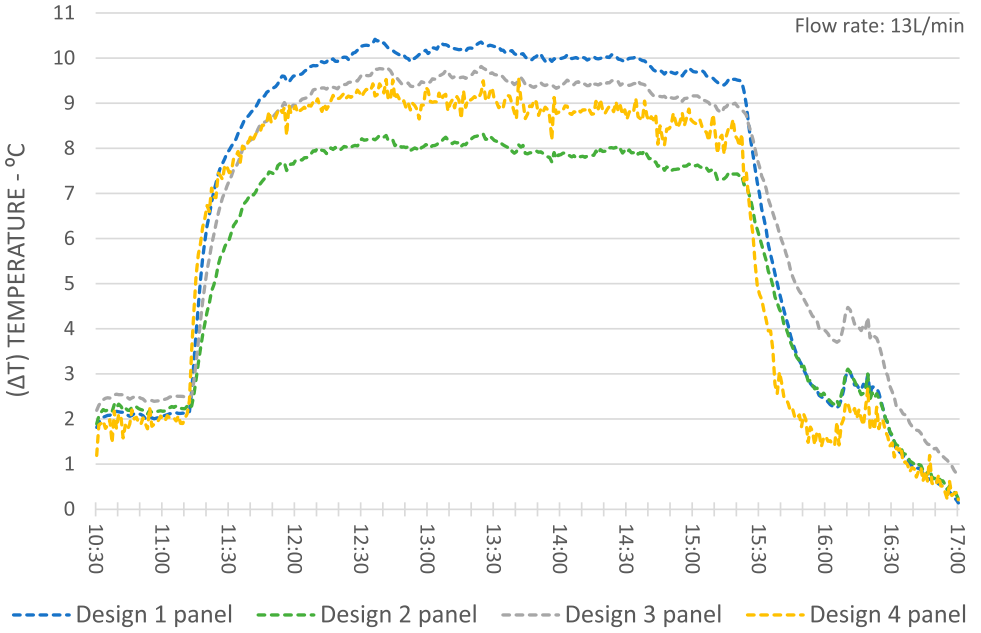

Figure 13. The difference between the panel surface and the ambient operative temperature.

each other while Design 2 heat fux reading is notably lower only reaching 65–70 W/m^2.

In terms of surface temperature, Figure 13 shows the temperature difference (ΔT) between the surface of the panels (T_S) and the ambient operative temperature (OT_i). As previously mentioned, the higher this temperature difference, the higher the heat flux. The result again demonstrated consistency in the order of the thermal performance for each panel design, under the different ambient conditions. Design 1 achieved a surface temperature 10°C lower than the ambient temperature, followed by Design 3 and Design 4 respectively. As expected, Design 2 has the highest surface temperatures resulting in the lowest temperature difference.

5.2. Panels' structure thermal transmittance (U-value)

The total *U*-value (Thermal transmittance) of the panel radiant surface structure (*Ut*) is calculated based on Equation 4 (Equation 4). This calculation also assumes that the heat transfer between the water and the radiant surface is equal to the heat flux between the radiant surface and the conditioned room. To avoid lagging in sensor readings, the temperatures of the radiant surface and average panel water temperature used for calculations are selected within one hour of when the heat flux reaches, and is stable, at its maximum value. As the flow rate through the panel is relatively high, at about eight changes per minute, the average water temperature in the panels is relatively close to the inlet water temperature. The resulting *U*-value of the 4 panels throughout the test runs are averaged out and shown in Table 2.

Overall, Design 1 has the highest *U*-value, followed by Design 3, 4, and 2 respectively. The panels of Design 1 and 2 are built with similar materials and with similar weights but the *U*-value of Design 2 is much lower than that of Design 1. This indicates the flaws in Design 2 where a high thermal contact resistance reduces the heat transfer efficiency. Similarly, the metal sheet radiant surface of Design 4 is supposed to have high Uvalue yet the panel structure *U*-value is only about 21 W/m^{2}k as the result of high thermal contact resistance caused by poor design.

Table 2. Structure *U*-value.

		Average structure *U*-value (W/m^{2}k)				
Design	Weight Kg	Test 1	Test 2	Test 3	Test 4	Average
1	6	31.26	30.79	34.22	33.83	32.52
2	6.5	11.67	13.12	14.01	13.99	13.2
3	10	22.60	24.03	26.18	25.99	24.7
4	3.5	21.76	19.41	20.85	21.73	20.92

5.3. Time constant

Figure 14 shows the mathematic time constant (TC) models for the four panels calculated using Equation (5) and based on the heat flux readings shown in Figure 12. Notably, for each panel, there are two values calculated for the time constant, one for the system commencing and the other for the system ceasing. The commencing time constant indicates how fast the panel can start or react to an active control command. The ceasing time constant shows how fast the panel can be fully deactivated.

Table 3 shows the time constant values along with panel weight and *U*-value. Interestingly, the time constant especially the commencing time constant of a specific panel design is not stable, instead can widely vary between tests. Note, in all of the tests the water flow rate is kept at 13 L/minute while various ambient temperatures and inlet water temperatures were recorded. Nevertheless, there is consistency in terms of the order of the time constant of the panel designs. In both commencing and ceasing, Design 4 has the lowest time constant (i.e. fastest response), followed by Design 1 in second place. Design 2 has the highest commencing time constant (slowest to start), but Design 3 has the highest ceasing time constant (slowest to stop).

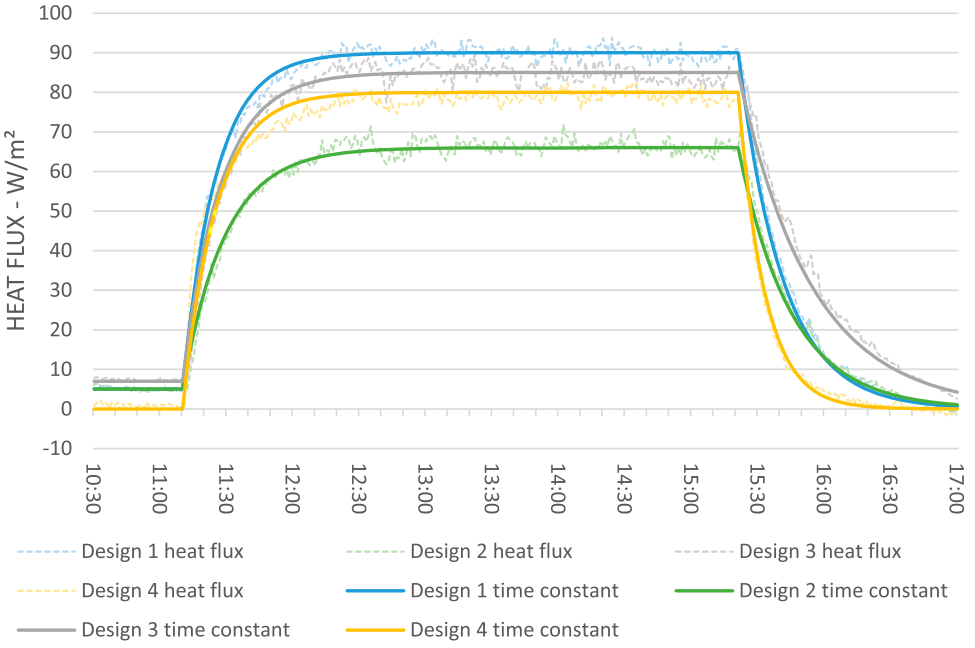

Figure 14. Time constant model of the four ceiling panel designs.

Table 3. Time constant.

			Initiation Time Constant (minutes)				Cool-down Time Constant (minutes)			
Design	*U*-value W/m²k	Weight	Test 1	Test 2	Test 3	Test 4	Test 1	Test 2	Test 3	Test 4
1	32.52	6 kg	8	12	15	12	21	23	20	20
2	13.2	6.5 kg	15	17	19	15	23	27	24	20
3	24.7	10 kg	12	15	17	13	35	37	33	27
4	20.92	3.5 kg	7	10	15	9	10	13	12	9

Table 4. Experiment-derived heat transfer coefficients.

		Average **Total** heat transfer coefficient (h) W/m²K				Average **Convective** heat transfer coefficient (h_c) W/m²K			
Design	**Radiant** heat transfer coefficient (h_r) W/m²K	Test 1	Test 2	Test 3	Test 4	Test 1	Test 2	Test 3	Test 4
1	5.5	9.6	9.1	8.95	8.6	4.1	3.6	3.45	3.1
2		9.35	8.75	8.55	8.2	3.85	3.25	3.05	2.6
3		9.65	9.05	8.95	8.5	4.15	3.55	3.45	3
4		9.7	9	8.85	8.3	4.2	3.5	3.35	2.8

5.4. Heat transfer coefficient

The Total heat transfer coefficient (h) and the Convective heat transfer coefficient (h_c) are calculated based on Equations (1) and (2). The values for the ambient operative temperature (OT_i), surface temperature (T_S), and heat flux (q) used in the calculations are the average values over a one-hour period after the heat flux reaches its maximum and is therefore stable. The results are shown in Table 4.

6. Discussion

6.1. Thermal performance comparison and design effects

Overall, all of the panels are dynamic and fast in responding to control commands, indicating time constants of all four panels between 7–19 min. In comparison, commercially available radiant panels generally have a time constant between 30–91 s, while the time constant varies between 0.25–3.5 h for embedded (heavyweight) systems (Ning, Schiavon, and Bauman 2015). Hence, the time constant of designs 1, 2, and 3 can be considered fast for ESS, while design 4 is slower.

Interestingly, the simulation of Ning, Schiavon, and Bauman (2015) indicates that configuration aspects such as pipe spacing, or material of the radiant surface, dominate the time constant of a radiant panel, rather than water temperature or flow rate. However, the empirical experiments conducted by Ye, et al (Ye et al. 2021) show that water temperature or flow rate can have notable impacts on the time constant of radiant panels. In this study, where the flow rate is the same across all tests, the changes in the time constant between tests indicate the possible impacts of other aspects, such as inlet water temperature, or room operative temperature, on the time constant of radiant panels. This could also explain why the values of the ceasing time constant are higher than that of the commencing time constant.

Although Design 4 is much lighter than Design 1, the commencing time constant values of the two panels are relatively close. Design 1 has a higher *U*-value than Design 4 allowing faster and higher heat transfer and enabling it to cool higher thermal

mass in a shorter time due to its high thermal transmittance (*U*-value). Contrarily, the ceasing time constant of Design 4 is 55% lower than that of Design 1. Similarly, Design 3 is heavier but has a much higher *U*-value than Design 2, resulting in a shorter commencing and longer ceasing time constant for Design 3.

Our results indicate that the time commencing constant is affected by both the U-value and thermal mass. In this stage, water is pumped through the capillary mat and the heat transfer is mainly between the water and the room through the panel structure. Here, high thermal transmittance (U-value) and low thermal mass will promote faster heat transfer resulting in shorter time constant values.

However the 'ceasing' time constant is mostly dictated by thermal mass, so the heavier panels will have a higher time constant. This is because, when the system is turned off, water is not pumped through the panels, and heat transfer is reliant upon the heat capacity stored in the panels' structure and the water contained in the capillary tubes. In our panels, the capillary tube mat used can store 0.45 Kg of water, which is relatively low when compared to the thermal mass of other radiant structures. Hence, when ceasing, the main heat transfer is between the room and the radiant capacity of the panel.

The overall panels' performance, in terms of heat flux and surface temperature, clearly indicates that all the designs are capable of providing radiant conditioning. Also, the consistency in the order of panel performance indicates the superior panel design. More experiments are required to further investigate the effect of panel design, system operation, and external conditions on panel performance, especially in terms of response time and improving heat transfer.

6.2. Heat transfer coefficient

The total heat transfer coefficient for the panels ranges from 8.1–9.7 W/m^{2}K. The differences in the heat transfer coefficient between tests can be explained by the variations in the convective heat transfer coefficient. This can be explained by the uncertainty in air velocity (which was not monitored) within the test environment, a large shed. Although the shed protects the experiment from external conditions to an extent, its large volume and high air leakage can promote internal air movement thus affecting the convective heat transfer. Yet, the results for the total heat transfer coefficient are within the range of 8–10 W/m^{2}K suggested by several previous studies (Shinoda et al. 2019), although lower than the 11 W/m^{2}K recommended by the RHEVA handbooks or 10.8 W/m^{2}K of standard EN1264-5 for large open spaces (Shinoda et al. 2019). The results for the total heat transfer coefficient values of all four panels are relatively close to each other with a maximum deviation of approximately 4.5%. This is expected as the panel construction type has little impact on the total heat transfer coefficient. However, the temperature of the radiant surface of the four panels varies, yielding higher or lower heat transfer.

6.3. Application

Through the design and prototyping, Design 2 and Design 4 were simpler to construct while Design 1 and Design 3 were more complex. Routing the grooves for the capillary tubes in Design 1 is time-consuming and requires a high-end CNC machine while Design 3 is built with wet mortar which takes time to cure. The panels are also designed for *T*-frame suspended ceiling systems hence they fit the frame and can be installed with ease. Aside from Design 3 which is 10 kg, other panels are lightweight (3.5–6.5 kg) and are therefore more likely to meet the requirements of allowable weight.

7. Conclusion

In this research, four prototype hydronic radiant panels were constructed and instrumental experiments were conducted to assess their thermal response times, energy transfer, and resulting surface temperature. The following conclusions can be drawn from the empirical experiment.

(1) While all of the prototypes are proven to be capable of functioning as radiant panels, the prototype of Design 1, with capillary tubes embedded in routed plasterboard ceiling tile, yields the best result. Flaws in Design 2 and 4, demonstrate poor connection between capillary tubes and the ceiling tile, notably hindering their performance.
(2) Our experiments indicate total heat transfer coefficient values are in the range of 8–10 W/m^{2}K, similar to established studies yet less than the total heat transfer coefficient of 11 W/m^{2}K reported by the RHEVA handbook or the 10.8 W/m^{2}K of the EN1264-5 standard.
(3) The thermal connection between the capillary tube mat and the radiant surface has notable impacts on the thermal performance of the panel. Panels, where the tubes are embedded within the delivering surface material, perform best regarding heat transfer and surface temperature. The thermal connection in Design No.1 and No.3 is better than that of panels 2 and 4 resulting in higher *U*-value and superior heat transfer.
(4) While the time constant may reflect the design and material of a panel, operation conditions such as water temperature, flow rate, or operative temperature may have a notable effect on how fast the system responds. It cannot be assumed that the commencing and ceasing time constants will be equal. Nevertheless, in reflection upon the title of this paper, we are demonstrating highly responsive and dynamic radiant panel systems.
(5) The prototype panels were also designed for modularity, ease of installation, and architectural aesthetics. The prototypes can relatively easily replace existing ceiling tiles on suspended grid ceiling systems making them ideal for retrofitting existing offices and commercial buildings. However, the production of routed and wet capillary panels (Design 1 and Design 3) is time-consuming and befouling. Therefore, panel designs that are thermally effective but easier to produce will be explored.

Since our initial testing, two more panel designs have been developed, exploring 'non-routed' nor wet panel designs. The thermal performance of such prototypes will be investigated and compared with the panels of this research. Furthermore, a 'Testcell' (an 18 m^2 room) emulating the conditions of a perimeter office room will be applied in the future testing of our panels.

The test chamber will provide an environment for realistic solar irradiation exposure, emulating Australian conditions. Instrumental experiments will be conducted within this 'Testcell' to establish the best panel designs. It is anticipated to report these findings in subsequent publications.

Disclosure statement

No potential conflict of interest was reported by the author(s).

References

Anderson, T., and M. Luther. 2012. "Designing for Thermal Comfort Near a Glazed Exterior Wall." *Architectural Science Review* 55 (3): 186–195. https://doi.org/10.1080/00038628.2012.697863.

Anderson, T., M. Luther, and T. Brain. 2011. "Assessment of Thermal Comfort Near a Glazed Exterior Wall." In *ANZASca 2011: From Principles to Practice in Architectural Science: Proceedings of the 45th Annual Conference of the Australian and New Zealand Architectural Science Association*, 1–10. ANZAScA.

Babiak, J., B. W. Olesen, and D. Petras. 2007. Low Temperature Heating and High Temperature Cooling: REHVA GUIDEBOOK No 7.

Bulut, M. B., S. Wilkinson, A. Khan, X.-H. Jin, and C. L. Lee. 2021. "Thermal Performance of Retrofitted Secondary Glazed Windows in Residential Buildings–Two Cases from Australia." *Smart and Sustainable Built Environment* 11 (4): 1182–1192. https://doi.org/10.1108/SASBE-03-2021-0050.

Cholewa, T., R. Anasiewicz, A. Siuta-Olcha, and M. A. Skwarczynski. 2017. "On the Heat Transfer Coefficients Between Heated/Cooled Radiant Ceiling and Room." *Applied Thermal Engineering* 117:76–84. https://doi.org/10.1016/j.applthermaleng.2017.02.019.

Díaz, N. F., and C. Cuevas. 2010. "Testing and Thermal Modeling of Radiant Panels Systems as Commissioning Tool." *Energy Conversion and Management* 51 (12): 2663–2677. https://doi.org/10.1016/j.enconman.2010.06.001.

Ding, P., Y. Li, E. Long, Y. Zhang, and Q. Liu. 2020. "Study on Heating Capacity and Heat Loss of Capillary Radiant Floor Heating Systems." *Applied Thermal Engineering* 165:114618. https://doi.org/10.1016/j.applthermaleng.2019.114618.

Do, H. Q., M. B. Luther, M. Amirkhani, Z. Wang, and I. Martek. 2022. "Radiant Conditioning Retrofitting for Residential Buildings." *Energies* 15 (2): 449. https://doi.org/10.3390/en15020449.

Do, H. Q., M. Luther, J. Matthews, and I. Martek. 2022. *Optimizing Conditioning Systems in the Perimeter Zones of Office Buildings*. ASA 2022: Building on Knowledge, Theory and Practice: Proceedings of the 55th Annual Conference of the Architectural Science Association, Architectural Science Association.

Feng, J. D. 2014. *Design and Control of Hydronic Radiant Cooling Systems*. Berkeley: Department of Architecture, University of California.

Gallardo, A., and U. Berardi. 2022. "Experimental Evaluation of the Cooling Performance of Radiant Ceiling Panels with Thermal Energy Storage." *Energy and Buildings* 262:112021. https://doi.org/10.1016/j.enbuild.2022.112021.

Imanari, T., T. Omori, and K. Bogaki. 1999. "Thermal Comfort and Energy Consumption of the Radiant Ceiling Panel System." *Energy and Buildings* 30 (2): 167–175. https://doi.org/10.1016/S0378-7788(98)00084-X.

Jing, Z., and L. Jiayu. 2020. "Study on Heat Transfer Delay of Exposed Capillary Ceiling Radiant Panels (E-CCRP) System Based on CFD Method." *Building and Environment* 180:106982. https://doi.org/10.1016/j.buildenv.2020.106982.

Li, R., T. Yoshidomi, R. Ooka, and B. W. Olesen. 2015. "Field Evaluation of Performance of Radiant Heating/Cooling Ceiling Panel System." *Energy and Buildings* 86:58–65. https://doi.org/10.1016/j.enbuild.2014.09.070.

Luther, M., O. Tokede, and C. Liu. 2020. "Applying a Comfort Model to Building Performance Analysis." *Architectural Science Review* 63 (6): 481–493. https://doi.org/10.1080/00038628.2020.1742645.

Miriel, J., L. Serres, and A. Trombe. 2002. "Radiant Ceiling Panel Heating–Cooling Systems: Experimental and Simulated Study of the Performances, Thermal Comfort and Energy Consumptions." *Applied Thermal Engineering* 22 (16): 1861–1873. https://doi.org/10.1016/S1359-4311(02)00087-X.

Morse, R. 1963. "Radiant Cooling." *Architectural Science Review* 6 (2): 50–53. https://doi.org/10.1080/00038628.1963.9696068.

Mosa, M., M. Labat, and S. Lorente. 2019a. "Constructal Design of Flow Channels for Radiant Cooling Panels." *International Journal of Thermal Sciences* 145:106052. https://doi.org/10.1016/j.ijthermalsci.2019.106052.

Mosa, M., M. Labat, and S. Lorente. 2019b. "Role of Flow Architectures on the Design of Radiant Cooling Panels, a Constructal Approach." *Applied Thermal Engineering* 150:1345–1352. https://doi.org/10.1016/j.applthermaleng.2018.12.107.

Ning, B., S. Schiavon, and F. S. Bauman. 2015. A Classification Scheme for Radiant Systems Based on Thermal Time Constant.

Residovic, C. 2017. "The New NABERS Indoor Environment Tool – The Next Frontier for Australian Buildings." *Procedia Engineering* 180:303–310. https://doi.org/10.1016/j.proeng.2017.04.189.

Rhee, K.-N., and K. W. Kim. 2015. "A 50 Year Review of Basic and Applied Research in Radiant Heating and Cooling Systems for the Built Environment." *Building and Environment* 91:166–190. https://doi.org/10.1016/j.buildenv.2015.03.040.

Rhee, K.-N., B. W. Olesen, and K. W. Kim. 2017. "Ten Questions About Radiant Heating and Cooling Systems." *Building and Environment* 112:367–381. https://doi.org/10.1016/j.buildenv.2016.11.030.

Shinoda, J., O. B. Kazanci, S.-I. Tanabe, and B. W. Olesen. 2019. "A Review of the Surface Heat Transfer Coefficients of Radiant Heating and Cooling Systems." *Building and Environment* 159:106156. https://doi.org/10.1016/j.buildenv.2019.05.034.

Teitelbaum, E., K. W. Chen, D. Aviv, K. Bradford, L. Ruefenacht, D. Sheppard, M. Teitelbaum, F. Meggers, J. Pantelic, and A. Rysanek. 2020. "Membrane-Assisted Radiant Cooling for Expanding Thermal Comfort Zones Globally Without Air Conditioning." *Proceedings of the National Academy of Sciences* 117 (35): 21162–21169. https://doi.org/10.1073/pnas.2001678117.

Xing, D., and N. Li. 2022. "Reconstruction of Hydronic Radiant Cooling Panels: Conceptual Design and Numerical Simulation." *Thermal Science and Engineering Progress* 30:101272. https://doi.org/10.1016/j.tsep.2022.101272.

Xing, D., N. Li, C. Zhang, and P. Heiselberg. 2021. "A Critical Review of Passive Condensation Prevention for Radiant Cooling." *Building and Environment* 205:108230. https://doi.org/10.1016/j.buildenv.2021.108230.

Ye, L., Y. Ding, C. Zhou, and J. Li. 2023. "Heat Exchange Pipe Spacing for Optimal Temperature Uniformity on Cold Radiant Ceiling Surfaces." *Energy and Buildings* 282: 112788. https://doi.org/10.1016/j.enbuild.2023.112788.

Ye, M., A. A. Serageldin, A. Radwan, H. Sato, and K. Nagano. 2021. "Thermal Performance of Ceiling Radiant Cooling Panel with a Segmented and Concave Surface: Laboratory Analysis." *Applied Thermal Engineering* 196:117280. https://doi.org/10.1016/j.applthermaleng.2021.117280.

Yin, Y., R. Wang, X. Zhai, and T. Ishugah. 2014. "Experimental Investigation on the Heat Transfer Performance and Water Condensation Phenomenon of Radiant Cooling Panels." *Building and Environment* 71:15–23. https://doi.org/10.1016/j.buildenv.2013.09.016.

Yu, G., and Y. Yao. 2015. "The Experimental Research on the Heating and Cooling Performance of Light Floor Radiant Panels." *Procedia Engineering* 121:1349–1355. https://doi.org/10.1016/j.proeng.2015.09.018.

Zhong, Z., W. Ma, S. Yao, X. Xu, and J. Niu. 2022. "Enhancing the Cooling Capacity of Radiant Ceiling Panels by Latent Heat Transfer of Superhydrophobic Surfaces." *Energy and Buildings* 263:112036. https://doi.org/10.1016/j.enbuild.2022.112036.